

Extracellular Hydrogen Peroxide Measurements Using a Flow Injection System in Combination with Microdialysis Probes – Potential and Challenges

Maria Moßhammer¹, Verena Schrameyer¹, Peter Ø. Jensen^{2,3}, Klaus Koren^{1,4*} and Michael Kühl^{1,5*}

¹ Marine Biological Section, Department of Biology, University of Copenhagen, Denmark

² Department of Clinical Microbiology, Rigshospitalet, Denmark

³ Department of Immunology and Microbiology, Costerton Biofilm Center, Faculty of Health and Medical Sciences, University of Copenhagen, Denmark

⁴ Department of Bioscience – Microbiology, University of Aarhus, Denmark

⁵ Climate Change Cluster, University of Technology Sydney, Australia

* Correspondence: mkuhl@bio.ku.dk, klaus.koren@bios.au.dk

ARTICLE INFO

ABSTRACT

Keywords:

Hydrogen peroxide
H₂O₂
ROS
Flow injection analysis
FIA
Microdialysis probe
Extracellular measurement
Optical sensor
Chemiluminescence

There is a strong need for techniques that can quantify the important reactive oxygen species H₂O₂ in complex media and *in vivo*. We combined chemiluminescence-based H₂O₂ measurements on a commercially available flow injection analysis (FIA) system with sampling of the analyte using microdialysis probes (MDPs), typically used for measurements in tissue. This allows minimally invasive, quantitative measurements of extracellular hydrogen peroxide (H₂O₂) concentration and dynamics. By coupling MDPs to the FIA system, measurements are no longer limited to filtered, liquid samples with low viscosity, as sampling via a MDP is based on a dynamic exchange through a permeable membrane with a specific cut-off. This allows continuous monitoring of dynamic changes in H₂O₂ concentrations, alleviates potential pH effects on the measurements, and allows for flexible application in different media and systems. We give a detailed description of the novel experimental setup and its measuring characteristics along with examples of application in different media and organisms to highlight its broad applicability, but also to discuss current limitations and challenges.

1. Introduction

Hydrogen peroxide (H₂O₂) is a reactive oxygen species (ROS) [1] and a strong oxidant, but due to its high activation energy H₂O₂ is relatively unreactive in comparison to other ROS [2]. The peroxide bond is nonetheless prone to cleaving due to heating, photolysis or contact with redox metals [2,3]. These cleaving reactions can form the highly reactive hydroxyl radical (OH•), which has a very low activation energy and is one of the strongest known oxidants [2,4]; thus it is very important to understand the production and degradation processes of H₂O₂ as one of the main sources of OH•. Furthermore, H₂O₂ is of great importance in cell biology, where it plays a key role in important biochemical processes such as oxidative stress and as a transmitter of redox signals [2,5]. However, the exact role of H₂O₂ is often not fully understood due to uncertainties in the determination of real concentrations *in vivo* [6].

Some organisms such as algae [7] or human granulocytes (PMN) [8] release H₂O₂, while most cells and organism can sense and respond to H₂O₂ in their environment [5,9]. In many systems it is, however, still not possible to determine exact concentrations or monitor actual H₂O₂ dynamics, due to a lack of suitable techniques [6,9]. In an environmental context, H₂O₂ is released as an oxidative stress response by e.g. algae [10–15] or corals harboring microalgal symbionts [6,16]. H₂O₂ can also be formed via different (photo)chemical pathways in lakes [17,18], rivers [19,20], rainwater [17,19,21–25], geothermal springs [26] and open ocean seawater [19,27–30], and H₂O₂ has even been measured in thousands of years old ice cores [31,32]. In humans, H₂O₂ has been measured in exhaled air [33–35], urine [36,37], blood [38–40] or ocular fluids [41], and it functions as an important signaling agent between cells [42]. Hydrogen peroxide has also been linked to various diseases such as neurodegenerative diseases, Alzheimer's or lung infections [33,43,44] underlining the concentration-dependent dual character of H₂O₂ as a both harmful and important compound in biological

systems. There is thus a strong need for methods that can quantify concentrations of H_2O_2 *in vivo* or under *in vivo*-like conditions with minimal sample manipulation. Such measurements are paramount for our understanding of the processes regulating the release and degradation of H_2O_2 in different environmental and biomedical systems.

Quantification of H_2O_2 is frequently attempted with optical techniques based on irreversible luminescent probes. Such approaches can be used to detect H_2O_2 via the luminescence intensity upon probe exposure giving valuable insights into hotspots and the presence of a species. However, correlating such changes in luminescence intensity to real H_2O_2 concentrations is difficult and often impossible [6]. A frequently used and well established technique for the determination of H_2O_2 in liquid samples is based on flow injection analysis (FIA) in combination with a H_2O_2 -specific chemiluminescent reaction (Figure 1) [6,19]. This approach enables dynamic H_2O_2 concentration measurements in retrieved samples in near real time, where FIA overcomes the issue of the irreversibility of the underlying reaction scheme. Typically, such FIA-based systems consist of a valve system, which can switch between two modes (load and injection), a peristaltic pump ensuring a continuous flow of sample and reagents, and a photomultiplier tube coupled to a mixing cell for sensitive detection of the chemiluminescence intensity caused by the reaction of a chemiluminescent reagent (CL reagent) with the analyte of interest. Different chemistries such as luminol with a Co(II) catalyst [17,29,45–47] or the acridinium ester (10-methyl-9-(*p*-formylphenyl)-acridinium carboxylate trifluoromethanesulfonate) [19,48–51] have been used for H_2O_2 detection. Both chemiluminescence reaction schemes are pH dependent and show cross-sensitivities to Fe(II), which can however be overcome by working with buffered solutions and addition of FerroZine™ to complex freely available Fe(II) [45,48]. Temperature effects have to be taken into consideration as well, as chemiluminescent reactions are temperature dependent [52]. Luminol-based measurements are also influenced by other analytes [45], while acridinium ester (AE) based measurements (employed in this the present study) show high specificity towards H_2O_2 [19]. Other FIA-based H_2O_2 detection approaches are reviewed elsewhere [6].

A major shortcoming of the overall FIA technique is its restriction to aggregate-free, liquid samples of low

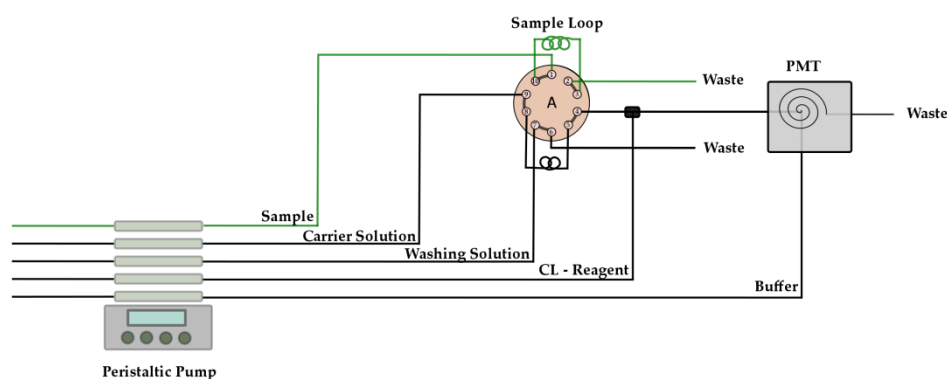


Figure 1: Schematic representation of a flow injection analysis (FIA) system used to quantify H_2O_2 in the load mode. The sample is acquired with a sample tube and filled in the sample loop. When switching to injection mode, the sample is mixed with the chemiluminescent reagent (CL) and flushed by the carrier solution into a mixing chamber, where it is mixed with a buffer solution to adjust the pH and facilitate the reaction with the chemiluminescent reagent. The mixing chamber is optically coupled to a photomultiplier tube (PMT) detector that monitors the analyte-dependent chemiluminescence signal. Even flow of sample and reagents is facilitated with a peristaltic pump.

viscosity, as connectors and tubes are very narrow and block easily. Thus, the sample often needs a pretreatment step, such as filtering. Additionally, a relatively large sample volume (up to a few mL) is typically required, which can impose dramatic changes and artefacts in systems with a restricted volume and limits the spatio-temporal resolution. To overcome these limitations, we combined the FIA system with sampling via so-called microdialysis probes (MDPs) (Figure 2). Such probes are minimally invasive as analytes are retrieved from the sample via diffusion across a microdialysis membrane with a defined molecular cut-off into a perfusion solution. MDPs consist of a semipermeable membrane, which can be used to dialyze liquid, semisolid or solid media [53]; they were first developed for minimally invasive *in vivo* measurements of drug concentrations in tissue and organs of animals or humans [54]. MDPs can be applied *in vivo* as well as *in vitro*; they have been frequently coupled to different analytical systems, such as liquid chromatography, flow-through biosensors and capillary and microchip electrophoresis [55] and also allow measurements beyond liquid samples [53].

The analyte recovery by the MDPs is dependent on various factors, such as MDP membrane length, perfusion speed of the internal carrier solution or temperature, making it a tunable system for specific applications with a variety of sampling schemes [54]. In combination with a dynamic measurement technique such as the FIA system, MDPs can thus facilitate flexible measurements in a range of media and systems. In this study, we give a detailed presentation of a MDP-

based FIA system for minimally invasive quantification of H₂O₂ concentration and dynamics. We give a detailed description of the novel experimental setup and its measuring characteristics along with different medical and biological applications to highlight its broad applicability, but also to discuss current limitations and challenges.

2. Materials and Methods

2.1. Chemicals and Stock Solution Preparation

10-Methyl-9-(phenoxyacetyl)acridinium fluorosulfonate (catalog number: 68617) (AE), hydrogen peroxide (H₂O₂) solution, 30 wt% (catalog number: 216763), catalase from bovine liver (catalog number: 1001937057), glucose oxidase from *Aspergillus niger* (catalog number: G7141-10KU), and FerroZine™ (catalog number: 160601) were purchased from Sigma Aldrich (sigmaaldrich.com). Na₂CO₃ was purchased from Riedel-deHaën (riedeldehaen.com; catalog number: 31432), HCl (37%) was purchased from Merck (merck-chemicals.com, catalog number: 1.01834.2500). The *Pseudomonas aeruginosa* strain used in this work was a catalase A negative PAO1 strain ($\Delta katA$) [56]. Luria-Bertani (LB) broth was prepared from 5 g L⁻¹ yeast extract (oxid.com; catalog number: LP0021), 10 g L⁻¹ tryptone-broth purchased from Oxoid (oxid.com; catalog number: LP0042), and 10 g L⁻¹ NaCl (merckmillipore.com; catalog number: 106404) at a pH of 7.5. F2 medium, i.e., an enriched seawater medium commonly used to culture marine microalgae, was prepared from filtered and autoclaved natural seawater supplemented with previously prepared stock solutions (final concentrations indicated in brackets): NaNO₃ (88.25 μ M), NaH₂PO₄ · H₂O (31.26 μ M), a trace metal stock solution containing (FeCl₃ (11.30 μ M), Na₂EDTA (12.97 μ M), CuSO₄ (0.040 μ M), Na₂MoO₄ (0.025 μ M), ZnSO₄ (0.077 μ M), CoCl₂ (0.077 μ M), MnCl₂ (1.430 μ M)), as well as vitamin stock solution containing thiamine-HCl (vitamin B1; 296.5 nM), biotin (vitamin H; 2.047 nM), cyanocobalamin (vitamin B12; 0.3689 nM). All ingredients for these solutions were purchased from Sigma Aldrich). Artificial Seawater (ASW) was prepared from de-ionized water (DI water) and probiotic reef salt, purchased from Aquaforest (aquaforest.eu) and mixed according to the manufacturer's instructions, where the final ASW had a salinity of 35. The ASW was autoclaved before usage. MilliQ water, DI water and other carrier solutions were treated with 3 mg catalase L⁻¹ for at least 30 minutes before further use, and were used to make all solutions. HCl as well as Na₂CO₃ and AE stock solution were added after the treatment of the DI water with catalase (3 mg L⁻¹, left for at least 30 minutes) to make a 0.01 M HCl solution, the 0.1 M Na₂CO₃ buffer solution (pH ~11.3) and the AE solutions. In experiments where free Fe(II) was expected, FerroZine™ was added to the AE solution to a final concentration of 250 nM. H₂O₂ stock solutions were freshly prepared every day using untreated DI water.

2.2. Instrumentation

We used a flow injection analysis system (FeLume; Waterville Analytical) with the dedicated analysis software. The FIA system was coupled to a peristaltic pump (Dynamax, Rainin Instrument Company; shoprainin.com) and a syringe pump (Aladdin, World Precision Instruments; wpiinc.com) using PVC pump tubes (Tygon R3607, red/red) obtained from Glass Expansion (geicp.com). The tubing in-between valves in the FIA system consisted of fluoropolymer tubing (Upchurch Scientific® FEP; idex-hs.com). Microdialysis probes (CMA 7 Metal Free, 2 mm membrane length, with a cut-off of 6 kDa) were purchased from CMA (microdialysis.se, reference number: 8010772) and handled according to the manufacturer's guidelines, flushing it with ethanol prior to the first usage. Measurements of O₂ concentration were done with a FireStingGO₂ meter in combination with an OXR430 fiber-optic O₂ sensor or a respiration vial equipped with an O₂ sensor spot (OXVIAL20) that was monitored via the transparent glass wall of the vial with a bare fiber connected to the meter; all items were obtained from Pyroscience (pyro-science.com). Electrochemical measurements of H₂O₂ were done with a H₂O₂ microsensor (ISO-HPO-100) coupled to a free radical analysis system (both obtained from World Precision Instruments; wpiinc.com). Solutions were filtered through syringe filters (Whatman, 0.02 μ m, 10 mm; Anato™ 10, gelifesciences.com; catalog number: 6809-1102). Samples were illuminated with a fiber-optic tungsten-halogen lamp equipped with a branched flexible light guide (KL1500, Schott.com), and incident light levels (400-700 nm) for different lamp settings were quantified in the samples with a submersible, spherical mini quantum sensor (US-SQS/L) coupled to a calibrated quantum irradiance meter (ULM-500) both purchased from Walz (walz.com).

2.3. Flow Injection Analysis (FIA) System Combined MDPs

The commercially available FIA system has a 10-port valve, which can be switched between load mode and injection mode (Figure 2) via the PC-controlled software. The system can be set up to also include a washing loop (e.g. diluted HCl) in order to clean the system tubings; this is e.g. relevant when using seawater in order to dissolve precipitates formed during the measurement [57]. The chemistry and chemiluminescent reaction for H₂O₂ measurements was described by King et al. [58]. Briefly, the chemiluminescent acridinium ester reagent (AE) reacts irreversibly with H₂O₂ forming an instable dioxetane complex, which releases energy in the form of light upon degradation to *N*-methylacridone under alkaline conditions. The chemiluminescence is detected by the PMT as a signal peak for a particular sample. In order to not over-saturate the PMT, signal intensities above ~1 million counts were avoided by adjusting the concentration

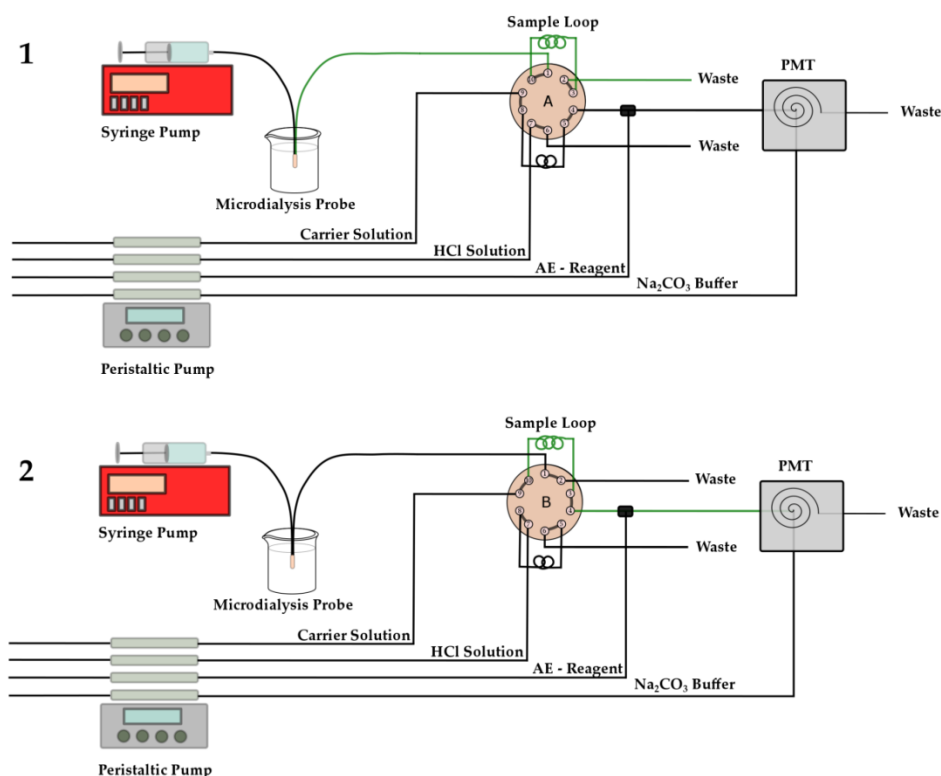


Figure 2: Load and injection mode of the FIA system coupled with the microdialysis probe (MDP). 1) Load mode. H₂O₂ is sampled via the microdialysis probe and guided into the sample loop. Excess solution will be flushed into the waste. Once the sample loop is filled, the 10-port valve can be switched to 2) injection mode. The sample solution containing H₂O₂ is flushed out of the sample loop, is mixed with the acridinium ester (AE) reagent and then transported into the detector mixing chamber by the carrier solution (such as catalase treated MilliQ water or seawater), where it is mixed with a buffer solution adjusting the pH. The microdialysis probe is operated by a syringe pump, where different speeds can be set. All other solutions (carrier solution, HCl solution / acid wash, chemiluminescent reagent (acridinium ester) and the Na₂CO₃ buffer are pumped through the system using a peristaltic pump.

of the chemiluminescent reagent. The peak integral can then be correlated – after prior calibration – to a specific H₂O₂ concentration. The MDPs allow the diffusive exchange of the analyte between the external sample medium and the inner, analyte-free probe perfusion medium, which are separated by a microdialysis membrane, with a specific molecular cut-off. A perfusion fluid (untreated DI water) is pumped through the dialysis probe at a certain speed, and is then transported into the 20 cm long sample loop of the flow injection system. The inner diameter (ID) of the FEP tubing used for the sample loop is 0.75 mm, which means the minimal sample volume is 88.4 μL (a small excess is however recommended to make sure the loop as well as the connectors are filled with bubble free sample solution). The sample loop is then flushed out by a catalase treated carrier solution, mixed with the AE reagent and transported into the reaction chamber in front of the PMT, where the pH is adjusted by a buffer solution (0.1 M Na₂CO₃, pH ~11.3). Switching back to ‘sample mode’ flushes the system with HCl (0.01 M) to keep the system from clogging due to precipitates (Figure 2.2).

2.4. Calibration With and Without MDPs

Calibration of the FIA system without the MDP connected (Figure 3A and Figure 4A) were done by adding defined volumes of the H₂O₂ stock solution (made in DI water) to the measurement medium. The same medium was used as carrier solution but treated with 3 mg L⁻¹ catalase and filtered if necessary. For calibrations with the MDP connected to the FIA system (Figure 3A and Figure 4B), the perfusion-fluid pumped from the syringe through the MDP was untreated DI water, while DI water treated with 3 mg L⁻¹ catalase was used as a reagent carrier solution and calibration solutions were stirred. As H₂O₂ has to enter the MDP via diffusion, a diffusion boundary layer establishes around the probe making it sensitive to stirring. The H₂O₂ stock solution was made in DI water and added to the stirred sample medium. For calibrations at elevated temperatures, vials containing the medium were heated to the required temperature, and H₂O₂ was only added right before measurement to avoid loss due to degradation. Real zero values were determined by adding catalase to a medium blank. The limit of detection (LOD) and limit of quantification (LOQ) were determined according

to literature [59,60] by taking 3.3 times the standard deviation of the catalase treated blank divided by the slope of the calibration curve (LOD; equation 1) or 10 times the standard deviation of the catalase treated blank divided by the slope of the calibration curve (LOQ; equation 2).

$$\text{LOQ} = \frac{3.3 * \sigma}{k} \quad (1)$$

$$\text{LOQ} = \frac{10 * \sigma}{k} \quad (2)$$

Where σ is the standard deviation of the catalase treated blank ($n = 3$) and k is the slope of the calibration curve.

2.5. Enzymatic Reaction Measurements

The experiment was conducted at room temperature in 200 mL of a stirred PBS buffered, glucose solution (1 mM), wherein H_2O_2 and O_2 were measured simultaneously (Figure 5) using a similar protocol of enzyme addition as in Koren et al. [61]. The sample solution was kept in a container sealed with a rubber stopper, to avoid O_2 leakage. The rubber stopper had three holes, one for the O_2 sensor, one for the MDP mounted on a glass rod, and one for the addition of the chemicals, which was sealed in-between reagent additions. Glucose oxidase (GOX) and catalase stock solutions were prepared in DI water (5 mg mL^{-1}). After baseline measurements, 0.125 mg GOX was added. The reaction was followed for 30 minutes. Then 0.125 mg catalase was added and the reaction was followed for 20 minutes. 0.250 mg GOX was added and the reaction monitored for 15 minutes. 0.500 mg catalase was added and the reaction followed for 15 minutes. Finally, 0.250 mg GOX was added together with additional 1mM glucose, and the reaction was followed until O_2 was consumed completely and no more H_2O_2 was produced. O_2 input via the MDP membrane was tested for in Figure S3.

2.6. H_2O_2 Dynamics in Light Stressed Sea Anemones

The sea anemone *Exaiptasia pallida* (strain H2) was transferred to a beaker containing aerated artificial seawater heated to 32°C . The organism was first kept in the dark for 60 minutes, while monitoring H_2O_2 (Figure 6) and O_2 levels. Subsequently, the sea anemone was exposed to high light ($\sim 1500 \mu\text{mol photons m}^{-2} \text{ s}^{-1}$; 400-700 nm) by irradiation from the side and top with a 2-branch flexible light guide connected to a fiber-optic tungsten-halogen lamp (KL1500, Schott). After ~ 80 minutes, the MDP was positioned in closer proximity to the animal than in the first position. The H_2O_2 build up due to light stress was followed for approximately 1 hour.

2.7. H_2O_2 Levels in LB Medium

The bacterium *Pseudomonas aeruginosa* was grown overnight at 37°C in an Erlenmeyer flask shaken at 170 rpm. Three falcon tubes were filled with 20 mL autoclaved and diluted LB medium (4mL LB + 16 mL DI) heated to 37°C and stirred within a heating block to ensure constant temperature. One tube was used to monitor H_2O_2 dynamics using the MDP - FIA system. The second tube was used to measure O_2 dynamics using a FireStingGO2. Every 10 minutes during the experiment, 1 mL samples were taken from this second tube, filtered via a $0.02 \mu\text{m}$ syringe filters (Whatman) into Eppendorf tubes and stored at 4°C over-night before measuring their H_2O_2 content via direct injection (FIA without a MDP) the following day. The third falcon tube was used to measure O_2 and H_2O_2 dynamics simultaneously using an electrochemical microsensor (ISO-HPO-100) coupled to a free radical analysis system (World Precision Instruments; wpiinc.com). Results are shown in the SI (Figure S2)). 2 mL of bacterial overnight culture were added to each of the stirred diluted LB media (37°C) resulting in a final density of approx. $2 \times 10^8 \text{ CFU mL}^{-1}$. H_2O_2 and O_2 concentrations were monitored for 2 hours.

3. Results

We present the measuring characteristics of the combined MDP-based FIA measurement of H_2O_2 , and illustrate various measurements optimization steps regarding reagent concentrations, syringe pump speeds and choice of sample media. The design of the set-up allows minimally invasive sampling without removing sample volume, which enables a wide variety of application in environmental and biomedical science. We demonstrate the application of the combined MDP-FIA system for minimally invasive measurements of H_2O_2 dynamics in almost real time.

3.1. Calibration

In the commercially available FIA system, the aggregate-free sample is sampled via a tube and then guided through a FEP tube alongside the carrier, the buffer, the HCl wash and the AE solution. They are transported via the peristaltic pump with the same pump speed through the valve system – to avoid differences in pressure (e.g. buildup of backpressure) within the system and to secure even flow speeds. A calibration curve of the ‘direct injection’ method (DI) is depicted in Figure 3A (black), using a 1 nM AE solution, a 0.1 M Na₂CO₃ buffer at pH 11.3, a 0.01 M HCl wash and MilliQ as carrier. All reagents were pre-treated with catalase according to literature [58] as described in the methods section. H₂O₂ standard solutions were prepared in untreated DI water and diluted in the measurement medium. In comparison, 2 calibration curves are depicted for the measurement with a MDP coupled to the FIA system (Figure 3A, blue and green). Sampling via a MDP connected to the FIA system (MDP-FIA) decreased the signal intensities, as the analyte recovery is

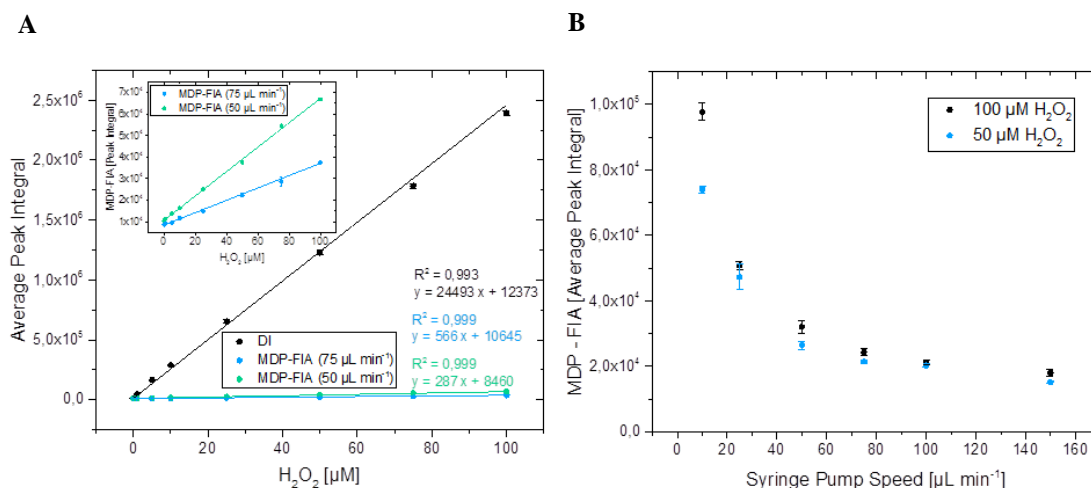


Figure 3: Comparison of H₂O₂ calibration curves measured with direct injection (DI) into the FIA system and via a microdialysis probe (MDP) coupled to the FIA system (MDP-FIA). A) Shows the difference between calibrating with MDPs (blue and green) and without MDPs (black, n=3). The inset shows the effect of the syringe pump speed on the calibration curve using MDPs. The two shown pump speeds are 75 µL min⁻¹ (blue; n=3) and 50 µL min⁻¹ (green; n=1). B) Shows the decrease in in signal intensities between DI and MDP-FIA measurements, by plotting the ratio of the Peak Integral of the DI signal divided by the Peak Integral of the MDP-FIA signal at the respective pump speed for different H₂O₂ concentrations. C) Shows the effects of the syringe pump speed on the analyte recovery determined for two different H₂O₂ concentrations (n=3). The calibrations were conducted at room temperature, under stirring (for the MDP) and in DI water.

diffusion limited and strongly dependent on external factors such as the syringe pump speed and MDP membrane characteristics (Figure 3A and B).

The measurement time was mainly influenced by the syringe pump speed, which is responsible for filling the 20 cm long sample loop, with a volume of ~88.4 µL (Table S1). The time needed for the sample solution to reach the sample loop also needs to be taken into consideration and this depends on the used tubes, their IDs and lengths. In our setup, the volume before the sample loop was ~50 µL. Thus the system response time - the time needed between sampling and signal out-put - comprises the time required to fill the sample loop plus the tubes connecting the MDP with the sample loop. However, once a continuous reaction is monitored only the time required for flushing the sample into the detector and refilling the sample loop needs to be taken into account in between measurements. The time necessary for flushing the sample out of the sample loop and through the detector can be monitored by observing the signal peak in the analysis software. The time depends on the pump speed of the peristaltic pump (here 1.8 mL min⁻¹), the length of tubing in between the sample loop and the detector as well as the geometry and volume of the flow cell. In our set-up the operational flushing time of the system was ~30 – 35 seconds.

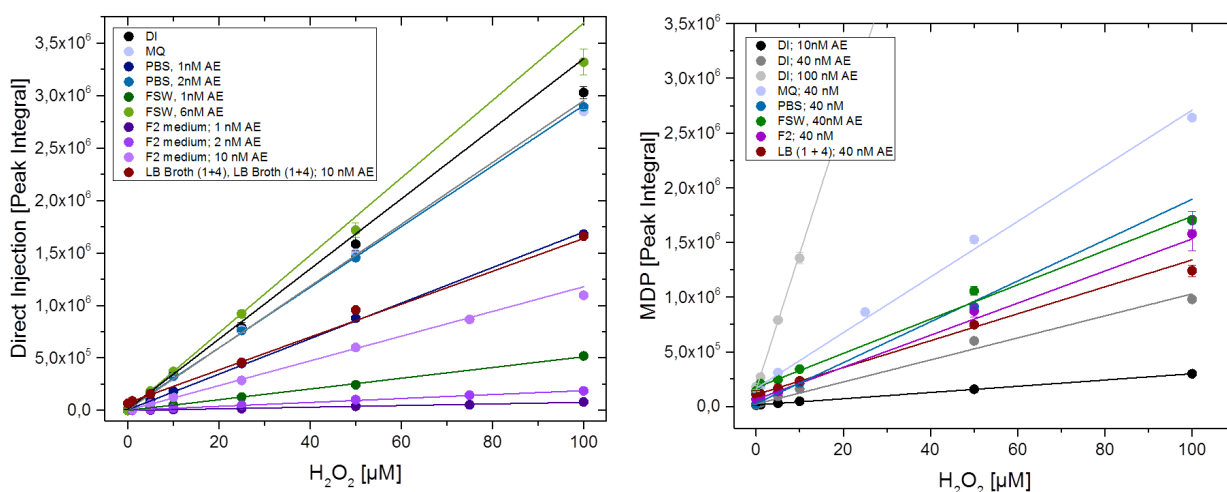


Figure 4: Effect of the chemiluminescent reagent (AE) concentration and the measurement medium composition on the H_2O_2 calibration curve as shown for DI water (black-grey), MilliQ water (light blue), PBS (blue), filtered seawater (FSW; green), F2 medium (purple), and LB broth (red). A) Calibrations via direct injection ($n=3$). B) Calibrations using a MDP for sampling ($n=3$).

It is well known [54] that the analyte recovery with MDPs depends on the syringe pump speed. Figure 3B shows the difference in analyte recovery over different pump speeds for a $100 \mu M$ and a $50 \mu M$ H_2O_2 solution for the MDP-FIA system. However, the slope of the linear calibration curves cannot only be modified by changing the syringe pump speeds, but also by changing the concentration of the AE reagent or the measurement medium (Figure 4A and B). We performed calibrations in DI water, MilliQ water, filtered seawater (FSW), artificial seawater (ASW), F2 medium, PBS and LB broth. The AE reagent concentration was gradually increased until signal intensities in comparable ranges could be achieved, in order to compensate for medium effects and the reduced analyte recovery caused by the MDP. The DI water used for preparing the H_2O_2 stock solution was untreated to avoid degradation of the calibration solutions prior to measurement and each measurement was repeated 3 times ($n=3$). H_2O_2 background values were determined by measuring in untreated blank medium and catalase treated medium samples.

Measurements of H_2O_2 using direct injection into the FIA or using the combined MDP-FIA set-up exhibited highly reproducible and linear calibration curves with small error bars for each particular setting of the various system parameters. If the system is switched off, it is however recommendable to recalibrate before measurement. Characteristics of the calibration curves in the different investigated media (shown in Figure 4) are given in Table 1 for the direct injection (DI) method as well as the MDP-FIA system, together with the used AE reagent concentrations aiming for an operational measuring range of $1 - 100 \mu M$. The slope, R^2 value as well as the determined LOD and LOQ are given. LOD (Equation 1) and LOQ (Equation 2) were determined according to literature [59,60]. The slopes allow a comparison between the different calibrations and chosen chemiluminescent reagent (AE) concentrations. It can be used to estimate the AE reagent concentration necessary to get a calibration curve of a certain steepness, which however does not oversaturate the PMT at higher H_2O_2 concentrations. Here we aimed for a slope of $\sim 1.2 \cdot 10^4 - 3 \cdot 10^4$ counts \cdot s per μM H_2O_2 for a calibration range between $1 - 100 \mu M$.

Table 1: Overview of calibration curve characteristics in different media at room temperature using direct injection (DI) or MDP-FIA (the same membrane was used for all measurements) based measurements at a range of acridinium ester (AE) reagent concentrations enabling a measurement range of 1-100 $\mu\text{M H}_2\text{O}_2$. k denotes the slope of the calibration curve, while σ is the standard deviation of the baseline, i.e. the signal measured in the catalase treated blank.

Medium	Injection Mode	AE reagent [nM]	Slope of the calibration curve (k) [counts · s · ($\mu\text{M H}_2\text{O}_2$) ⁻¹]	R ²	LOD (3.3* σ /k) [$\mu\text{M H}_2\text{O}_2$]	LOQ (10* σ /k) [$\mu\text{M H}_2\text{O}_2$]
DI water	DI	1	3.34*10 ⁴	0.994	0.05	0.14
	MDP-FIA	10	2.85*10 ³	0.999	0.56	1.7
		40	1.01*10 ⁴	0.980	0.15	0.47
		100*	1.24*10 ⁵	0.999	0.18	0.55
MilliQ water	DI	1	2.95*10 ⁴	0.997	0.03	0.08
	MDP-FIA	40	2.54*10 ⁴	0.996	0.16	0.49
PBS buffer	DI	1	1.69*10 ⁴	0.999	0.03	0.09
		2	2.89*10 ⁴	0.999	0.07	0.20
	MDP-FIA	40	1.87*10 ⁴	0.990	0.60	1.8
Filtered Seawater (FSW)	DI	1	5.11*10 ³	0.999	0.09	0.26
		6	3.69*10 ⁴	0.999	0.01	0.02
	MDP-FIA	40	1.57*10 ⁴	0.991	0.60	1.8
F2 medium	DI	1	7.84*10 ²	0.994	0.13	0.40
		2	1.87*10 ³	0.998	0.40	1.2
		10	1.18*10 ⁴	0.997	0.05	0.14
	MDP-FIA	40	1.47*10 ⁴	0.979	1.5	4.5
LB broth (1 + 4)	DI	10**	3.03*10 ⁴	0.999	0.02	0.06
		10	1.57*10 ⁴	0.998	0.05	0.14
	MDP-FIA	40	1.23*10 ⁴	0.997	0.71	2.2

* Calibration between 0 – 50 $\mu\text{M H}_2\text{O}_2$; signal intensities too high for 100 μM due to PMT saturation.

** Calibration temperature was 37 °C and it was calibrated between 0 – 25 μM .

3.2. Applications

We tested the combined MDP-FIA system in a range of different samples in order to demonstrate its broad applicability and to discuss some of the current limitations of this new H_2O_2 measurement approach. The microdialysis probe was successfully applied to monitor the enzymatic reactions of glucose oxidase and catalase in a PBS buffered glucose solution (Figure 5). The MDP-FIA system was also applied for measurements of H_2O_2 production due to light-induced, photo-oxidative stress within an important model organism in symbiosis research; the sea anemone *Exaiptasia pallida* that harbors photosynthetic microalgae as symbionts in its tissue [62] (Figure 6). The MDP-FIA approach has the advantage here, that it allows the positioning in close proximity to the animal / in the bulk water close to the animal, without the danger of accidentally attaching the tube to the moving animal due to the suction of the tube or blocking the tube by aggregates in the water. Figure 6 shows the difference the positioning of the MDP in relation to the animal makes concerning a stable signal output; especially in a bubbled system. Finally, we looked at H_2O_2 dynamics in a bacterial culture (Figure 7). Calibration measurements in several media show high background levels of H_2O_2 in the blank; especially the commonly used bacterial culture medium LB showed elevated levels of H_2O_2 after autoclaving. Therefore, we investigated how bacteria (in this case *Pseudomonas aeruginosa*) deal with the external H_2O_2 .

3.2.1. Enzyme reactions. Glucose oxidase (GOX) was added to 200 mL stirred, PBS buffered glucose solution (1mM) at room temperature, resulting in a decrease in O₂ concentration approximately correlating with the stoichiometrically expected increase in H₂O₂ concentration (Figure 5). The observed decrease in O₂ concentration (taking a ~ 6 minute delay due to loading times in account) was ~63 μM O₂ while the H₂O₂ concentration increased by ~57 μM H₂O₂. When adding catalase, the H₂O₂ concentration decreased again, while the decrease in O₂ concentration was slowed down due to the O₂ produced by the reaction of catalase and H₂O₂. When reaching anoxia, the H₂O₂ production stopped and a decrease towards 0 μM could be observed due to continuous catalase activity.

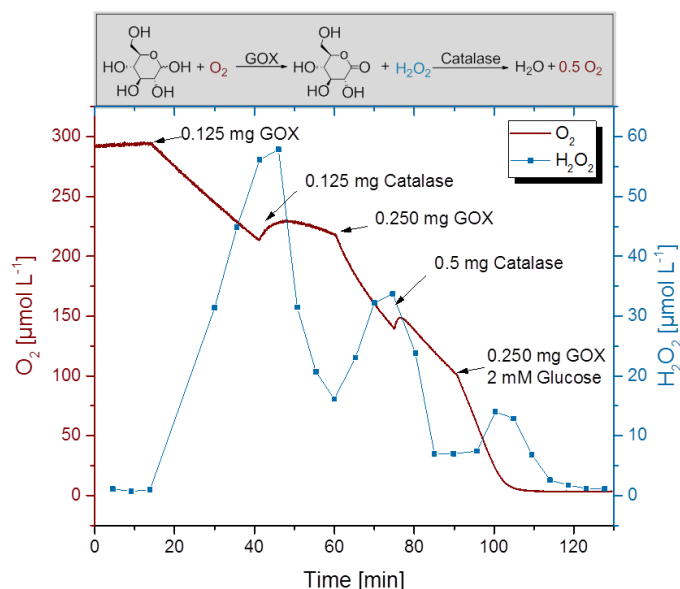


Figure 5: Monitoring of O₂ and H₂O₂ concentration dynamics in a PBS buffered 1 mM glucose solution upon alternating additions of glucose oxidase (GOX) and catalase. The enzymatic reaction schemes are shown above the data plot.

3.2.2. H₂O₂ dynamics in the sea anemone *Exaiptasia pallida*. The sea anemone was kept for one hour in darkness (Figure 6; grey) where there was a visible decrease in the background H₂O₂ concentration from ~ 1.3 μM to 0.6 μM. When switching to high light, an immediate increase in H₂O₂ concentration was observed. In one approach the MDP was placed in proximity to the moving anemone (>1 cm distance). In a second approach, the MDP was in close proximity to the tissue of one of the sea anemone's tentacles (<0.5 cm). H₂O₂ increased up to similar apparent steady-state

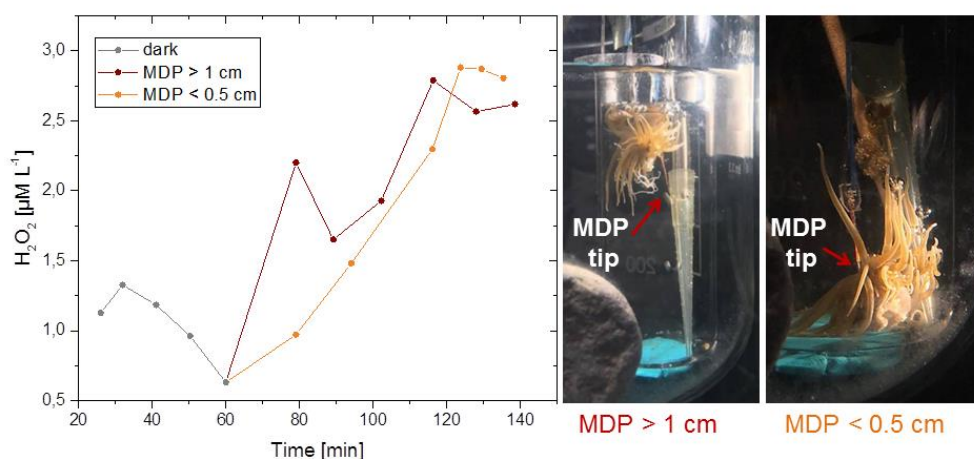


Figure 6: Monitoring of H₂O₂ dynamics at 32°C in the symbiont-bearing sea anemone *Exaiptasia pallida* in the dark (grey) and under light stress (~60 – 140 min) in two different measuring positions, with the MDP positioned >1 cm (orange) and <0.5 cm (yellow) from the tissue surface. The MDP was positioned in the bulk water surrounding the animal, but not in direct contact.

concentration in light of $\sim 2.7 \mu\text{M}$ in both positions. Measurements closer to the sea anemone tissue surface were less fluctuating.

3.2.3. H_2O_2 levels in LB medium. A solution of the bacterium *Pseudomonas aeruginosa* was pipetted into stirred, heated (37°C) LB medium (indicated at ~ 10 minutes in Figure 7), which was monitored by an optical O_2 sensor, while H_2O_2 was measured either via direct injection into the FIA or via a MDP inserted in the solution. Both H_2O_2 measurements via direct injection and via the MDP-FIA set-up showed a similar behavior, however, the direct injection measurement did not include blank values measured prior to bacteria addition. Therefore, the blank value of the calibration curve, which is LB medium without the addition of bacteria measured right before the experiment, is displayed to visualize the determined background concentration. The O_2 was depleted within 60 min, while the H_2O_2 concentration was depleted within 2-3 hours due to an apparent catalase activity in the bacterial solution. We note that the apparent blank value in the medium contained a significant amount of H_2O_2 , which was then consumed by the bacteria.

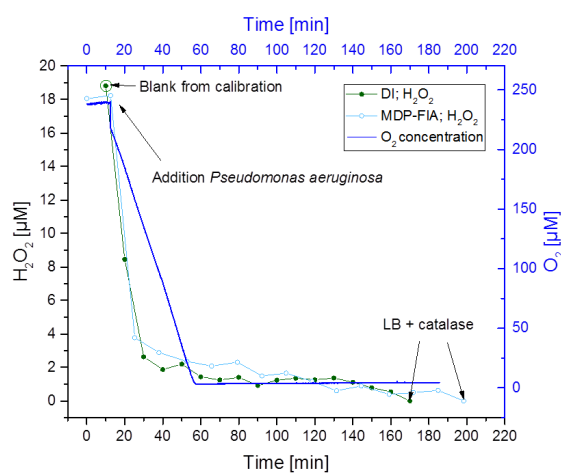


Figure 7: Monitoring of bacterial H_2O_2 and O_2 depletion in diluted, stirred LB growth medium at 37°C . The O_2 concentration (blue) was monitored by an optode, while H_2O_2 was measured with the combined MDP-FIA system (light blue) and with FIA system using direct sample injection (dark green). For the direct injection, the solution needed to be filtered ($0.02 \mu\text{m}$ syringe filter) and was stored at 4°C in the fridge overnight before measurement. For the direct injection (dark green), no sample was taken and filtered for the blank before the addition of the bacteria, the blank from the calibration is depicted instead.

4. Discussion

We developed a flexible measuring setup for quantifying the important reactive oxygen species H_2O_2 by combining sampling via microdialysis probes (MDPs) with sensitive chemiluminescence-based detection of H_2O_2 on a flow injection analysis (FIA) system. In its current configuration, the combined MDP-FIA based systems enables quantification of H_2O_2 in a variety of aquatic samples with high sensitivity (LODs and LOQs are shown in Table 1), linear calibration characteristics and a time resolution of ~ 4 min between measurements and ~ 6 minutes between samples. However, these system parameters can easily be modified e.g. by optimizing parameters such as the chemiluminescent reagent concentration, pumping speed of the system, tubing lengths and diameter, or choice of MDPs with different geometries and membrane characteristics. This system can now be used in a variety of environmental and biomedical samples.

As mentioned in the introduction, H_2O_2 can be found in natural waters. The formation of H_2O_2 in natural waters can be due to e.g. photochemical reactions of dissolved organic substances in the water [20]. However, background concentrations of H_2O_2 in other media, have to the best of our knowledge, not been studied in detail, especially when it comes to media used in the laboratory, such as DI water, MilliQ water, different seawater samples (ASW, FSW, F2 medium) or growth media used in microbiology such as LB-broth. To our knowledge, effects of water treatments such as autoclaving on the potential formation of background levels of H_2O_2 in liquid media have also not been studied. In order to determine such potential effects of media treatment and composition on H_2O_2 concentration a sensor system is required, which ideally allows continuous measurements in a broad variety of media. In liquid samples, the FIA system is well established as it allows continuous monitoring and can overcome pH interferences, which are often problematic for irreversible luminescent probes [6]. By combining the FIA system with a MDP we alleviated a major limitation of the FIA system, which is the need of pure samples. Small particulates such as cell or mineral aggregations or biofilms in the

sample can block the narrow tubes of the FIA system, posing a need for sample cleaning or filtration steps. This extra treatment can be avoided by the MDP-FIA system, as the MDP functions as a filter to substances larger than the specific molecular cut-off of the microdialysis membrane. Thus no aggregates can get into the sampling tube, while H₂O₂ enters the perfusion solution in the MDP via diffusion across the microdialysis membrane. This can also reduce the recovery of other potentially interfering species.

Due to its high activation energy, H₂O₂ is relatively stable and does not readily react with most biological molecules [2]. The basic mechanisms described in literature to be responsible for H₂O₂ decay in natural waters are enzymatic removal (biological) and abiotic chemical reduction [28]. The O-O bond itself is relatively weak and prone to homolysis caused by heating, radiolysis, photolysis or the presence of redox metals, such as iron or copper [2]. Both of these redox metals are for example present in seawater and are even enriched in F2 medium. Higher temperatures are also frequently employed, especially in medical applications. This can lead to an accelerated degradation of the H₂O₂ calibration solutions over time and needs to be taken into consideration as well when calibrating and measuring in different media.

4.1. Calibration. As long as the PMT in the FIA system is not saturated, the system sensitivity can be tuned by modifying the chemiluminescent reagent (AE) concentration, pump speed and MDP membrane length enabling a broad calibration range (here tested for concentrations between 1-10 μM and 1-100 μM). Lower AE concentrations allow a broader operational working range (Figure 4), whereas the use of higher AE concentrations can be used to measure H₂O₂ in the nM to μM ranges (Figure S1, Table 1). However, the increase in AE concentration increases the baseline as well. In theory, if the used solutions were completely H₂O₂ free, the baseline value should stay the same, but the FIA system is able to detect very low concentrations (in the pM range [19]) and thus the signal output can be influenced by residual amounts of H₂O₂. When catalase was added to the MilliQ or DI water (3 mg L⁻¹) used for the preparation of all solutions, the H₂O₂ background levels should be close to zero. This is however not true for the MDP perfusion-fluid which did not contain catalase to avoid degradation of the H₂O₂ diffusing into the perfusion fluid from the sample across the microdialysis membrane. It is also not true for the calibration standards, which contain the baseline H₂O₂ concentration of the specific medium. Such effects can be compensated for in the calibration procedure, by measuring in apparent zero H₂O₂ solutions before and after addition of catalase. This is necessary, as many real life systems can degrade H₂O₂ by releasing e.g. catalase, which then reacts with the background H₂O₂ as well as shown in our measurements in growth medium with bacteria (Figure 7). Therefore, it is important to know both the blank value and the real zero value in many applications when measuring H₂O₂.

4.1.1. Salt precipitation. Another issue, which needs to be considered is salt precipitation within the measuring system. At the working pH of ~11.3, seawater as well as F2 medium showed a white precipitate, most likely Mg(OH)₂ that is known to precipitate in seawater [49]. According to literature [1], the washing loop is sufficient to avoid excessive formation of the precipitate when working with seawater. However, as the combination with the MDP increased the loading time interval more precipitate formed, and the wash loop proved to be insufficient. Therefore, the pH buffer tube, as well as the AE tube were flushed with HCl instead during the loading step. 2-4 minutes prior to switching to the inject mode, the system was flushed again with the buffer and the AE solution to allow the baseline value to stabilize. This also has the benefit of less consumption of the AE solution.

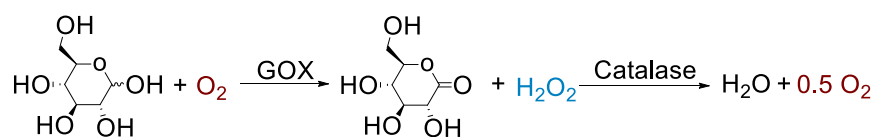
4.1.2. Syringe pump speed. Different syringe pump speeds were tested with a 2 mm long microdialysis probe membrane. However, the analyte recovery rate also depends on the MDP membrane length [54] and can thus be modulated by choosing MDPs with different dialysis membrane characteristics. With the MDPs having a 2 mm long membrane, pump speeds <50 $\mu\text{L min}^{-1}$ gave sufficient measuring signals for H₂O₂ without introducing excessive loading times of the FIA sample loop (Table S1). For this experiment (Figure 3B), relatively high H₂O₂ concentrations were chosen (100 μM and 50 μM), but it is apparent that highest signal differences could be detected at the lowest syringe pump speed, thus resulting in a lower H₂O₂ detection limit. Overall, for our applications we chose a pump speed of 25 $\mu\text{L min}^{-1}$, which correlates to an initial ~6 minute cycle to fill all tubes (this however, strongly depends on the tube length and diameter). After initial sampling, the following measuring cycles only depend on the time required to fill the sample loop, which for our set-up involved a loading time of ~4 minutes (20 cm long tubes, ID: 0.75 mm). This means there is a slight delay in the system, but the values can be correlated to the specific sampling interval if all the tube lengths and IDs are known, or experimentally tested.

4.2. Medium effects. We observed that the chemiluminescent signal and thus the apparent H₂O₂ level in different media can vary widely (Table 1, Figure 4). These effects were weak when comparing e.g. DI water to tap water, while e.g. a strong decrease in the detected signal was observed when switching from DI water to F2 medium or LB medium (Figure 4). These effects were strongest when using direct sample injection in the FIA system, where lower signals could e.g. be compensated for by increasing the AE reagent concentration. When using the combined MDP-FIA approach much less media effects on the chemiluminescent signal were observed and the same AE concentration could be used for all tested media in the MDP-FIA set-up. In the direct injection method, catalase treated medium was used as the carrier solution, which was directly mixed with the AE reagent and the buffer solution, and this resulted in more exposure to potentially interfering species. With the MDP-FIA set-up, the probe perfusion fluid is DI water (not the

catalase treated medium), and the membrane of the MDP together with the chosen perfusion speed reduces the recovery of not only H₂O₂ but also of potentially interfering species. In addition, the external carrier in the MDP-FIA set-up is catalase treated DI water, which means that no raw sample medium is injected into the system. This also alleviates precipitation from seawater, which is no longer injected into the system.

Depending on the sample medium, the observed changes in chemiluminescent intensity can have different reasons such as higher baseline concentrations of H₂O₂ in the medium, a slight change in pH or salinity, or the presence of transition metals reacting with the H₂O₂ added to the medium during calibration. The effect of changing from DI water to other media is shown in Figure 4A (DI) and Figure 4B (MDP-FIA) using identical settings and concentrations. Overall, some of the media effects can be attributed to precipitating salts from the artificial seawater and F2 medium, which affect the signal and can cause back pressure to build up in the system [49]. F2 medium also has a very high metal content. Cross-sensitivities of the AE reagent to other species (apart from Fe(II)) have not been reported to the best of our knowledge. However, testing for interferences by individual redox or transition metals and vitamins could give more insight into understanding the apparent drop in signal intensity. Higher baselines can be an indication for H₂O₂ present in the blank (e.g. LB broth; Figure 7), which can be compensated for by the addition of catalase. If the baseline decreases below the initial blank value after addition of catalase, the difference can be assumed to be due to the background H₂O₂ concentration for the given medium/solution. The cross sensitivity to Fe(II) was compensated for by the addition of FerroZine™ to the AE reagent. The FerroZine™ binds the Fe(II) before it can react with the AE solution. Ideally, the FerroZine™ would be directly added to the MDP perfusion - fluid reservoir in the syringe pump. However, we wanted to avoid FerroZine™ diffusion out of the MDP membrane into the sample. The addition of FerroZine™ to the carbonate buffer solution would be too late, as by then the reaction with the AE reagent would have already taken place. Therefore, adding FerroZine™ to the AE solution was the best choice. We conclude that irrespective of the various mechanisms causing such media effects, careful calibration and optimization for a given application alleviated the effects and resulted in highly linear calibration curves for H₂O₂.

4.3. Enzyme Reaction. The MDP was used in combination with an optical O₂ sensor to follow the reaction dynamics of glucose oxidase (GOX) and catalase in a PBS buffered glucose solution (Figure 5). Upon addition of GOX, glucose and O₂ reacted producing H₂O₂, as quantified by the combined MDP-FIA system. Upon addition of catalase the formed H₂O₂ was degraded according to the reaction Scheme 1.



Scheme 1: Enzymatic reaction of GOX with glucose in the presence of O₂ producing H₂O₂, which is subsequently degraded into O₂ and water upon addition of catalase.

This resulted in a temporary increase in O₂ concentration. However, as more O₂ was degraded than produced O₂ depletion was observed. The addition of GOX as well as catalase was repeated to demonstrate the capability of the MDP-FIA system to monitor dynamic H₂O₂ concentration changes. In the first addition step, the decrease in O₂ was higher than the increase in H₂O₂ probably due to the time delay between the FIA system response (6 minute cycle time) and the immediate response of the O₂ sensor. When looking at the O₂ signal 6 minutes prior to the addition of catalase the overall decrease in O₂ concentration was 63 μM, while the corresponding increase in H₂O₂ concentration was 57 μM, which was approximately in accordance with the reaction scheme stoichiometry. The combined MDP-FIA system is thus well suited to monitor dynamic H₂O₂ changes in solutions due to enzymatic reactions or other (bio)chemical processes. Such measurements are highly relevant in both environmental and biomedical sciences.

4.4. H₂O₂ Dynamics in the Sea Anemone *Exaiptasia pallida*. In a second application, we assessed the H₂O₂ production of the anemone *Exaiptasia pallida* (strain H2) under a global change relevant stress scenario [63], i.e., increased seawater temperature (32°C) and high irradiance (1500 μmol photons m⁻² s⁻¹). *Exaiptasia pallida* is commonly used in ecophysiological and biomolecular research as a model organism for cnidarian-coral symbioses [64], and technical advances in the assessment of quantitative H₂O₂ production of such organisms under oxidative stress are in strong demand. Besides the very first successful detection of light-stress induced H₂O₂ formation in *Exaiptasia*, we could also show that the positioning of the MDP has a direct effect on the signal quality. When the MDP was positioned >1 cm from the animal, significant fluctuation in the signal was observed and could be explained by the distance of the MDP to the anemone in connection to the weak mixing of the seawater via an air stone, which hampers an even build-up of H₂O₂ in the seawater surrounding the sea anemone. Additionally, bubbles could get trapped on the MDP membrane affecting H₂O₂ diffusion through the membrane. When positioning the MDP in closer contact with the anemone tissue (within the more stagnant water, i.e., the diffusive boundary layer surrounding the animal) more stable measuring signals were observed with a quasi-linear increase in signal over time once the MDP was positioned. The combined MDP-FIA system

thus enables spatially resolved measurements of H₂O₂ in open or closed systems containing living organisms, and this opens for a wide range of applications in the biological sciences, where O₂ respirometry is a core technique, which can now be easily combined with quantitative measurements of H₂O₂.

4.5. H₂O₂ Levels in LB medium. In a third application, the bacterium *Pseudomonas aeruginosa* was grown in diluted LB-broth medium. The autoclaved medium exhibited a high H₂O₂ background level (~17-18 μM in the diluted sample) causing a high baseline signal in the FIA. After addition of the bacteria, a drop in the signal intensity was observed due to catalase activity of the bacteria leading to H₂O₂ consumption. Such signal behavior was observed with direct FIA measurements of H₂O₂ as well as with FIA-MDP based measurements and measurements with an electrochemical H₂O₂ sensor (Figure S2). Such high H₂O₂ background levels were also confirmed by adding catalase to the reaction mixture (MDP-FIA) or to a LB medium blank, which was measured subsequently to finishing the experiment (DI). This illustrates the importance of careful assessment of background H₂O₂ levels in sample media, typically assumed to contain no H₂O₂. The autoclaved LB medium contained almost 20 μM H₂O₂, while non-autoclaved LB medium at room temperature showed a lower background concentration of ~ 4.9 μM H₂O₂ (Figure 4). This shows that the treatment of the sample medium can have an influence on background H₂O₂ concentrations and this needs to be evaluated before setting up an experiment. In addition, it indicates that media used e.g. for isolation and cultivation of bacteria may impose some oxidative stress if they contain such high H₂O₂ background levels. This result was rather unexpected and should be analyzed in more detail in the future. With proper calibration and quantification of background levels of H₂O₂ in apparent blank controls, the combined MDP-FIA system is an ideal instrument for such studies.

5. Conclusion

Coupling MDPs to a FIA system bypasses laborious sample cleaning and pre-treatment steps as well as consumption of the sample. It is possible to measure dynamic changes in H₂O₂ directly in complex sample solutions for extended time periods and without special sample treatment. It was possible to determine concentrations down to the sub μM range with good linear calibration curves. The set-up is highly tunable as the measurement range can be modified to enable broad calibration ranges (e.g. 1 – 100 μM) or highly sensitive measurements over a smaller operational range depending on the used MDP, the syringe pump speed, chemiluminescent reagent concentrations, or measurement temperature. Variation of the chemiluminescent (AE) reagent concentration allows a tuning of sensitivity and dynamic range of the H₂O₂ measurements that can compensate e.g. for a lower recovery when sampling H₂O₂ via the MDP membrane and/or at increased perfusion velocities of the carrier solution through the MDP. This tunability makes the MDP-FIA method a potent technique for H₂O₂ determination in many different samples and settings.

In this study we calibrated the combined MDP-FIA system within 1-10 μM and 1 – 100 μM (higher and lower was not tested; LODs depend on the measurement medium and the chosen settings) and optimize the syringe pump speed as well as reagent concentrations for different media and thus different applications. We successfully applied it to quantify the dynamics of H₂O₂ in solutions subject to enzyme reactions; we monitored H₂O₂ development in the sea anemone *Exaiptasia* under light stress, and quantified high background levels of H₂O₂ in autoclaved growth medium, which was consumed by the addition of bacteria. The combined MDP-FIA based system thus has a broad applicability for extracellular, near-real time H₂O₂ concentration measurements in both natural and defined samples. The method is minimally invasive, adjustable to different media and concentration ranges, and significantly reduces media effects in comparison to direct FIA-based measurements. While we have focused on H₂O₂ measurements in this study, the system can also be used for chemiluminescent reaction-based quantification of other chemical species [65–67] including ROS such as superoxide [68–70], where suitable chemiluminescent detection schemes have been described.

Acknowledgements

We thank Whitney King (Waterville Analytical) for his technical assistance and extensive advice on the use of the FeLume/FIA system. Sofie L. Jakobsen is thanked for technical assistance setting up the flow injection system. Kasper E. Brodersen is thanked for fruitful discussions. This study was supported by a Sapere-Aude (Grant No. DFF-1323-00065B) Advanced grant from the Danish Research Council for Independent Research | Natural Sciences (MK), a grant by the Danish Research Council for Independent Research | Technical and Production Sciences (MM, KK, MK, POJ) and an EU Marie Curie (Grant No. DENOCS H2020-MSCA-IF-2016-747464) Fellowship (VS).

Author Contributions

MM, KK and MK outlined the paper. Experiments were planned and conducted by MM, KK, VS and PØJ. Data analysis was done by MM, KK and VS. MM wrote the method paper with editorial input from VS, KK, PØJ and MK. All authors contributed to the final paper.

Conflict of Interest

The authors declare no conflict of interest. The founding sponsors had no role in the design of the study; in the collection, analyses, or interpretation of data; in the writing of the manuscript, and in the decision to publish the results.

References

1. Nathan, C.; Ding, A. SnapShot: Reactive oxygen intermediates (ROI). *Cell* **2010**, *140*, 8–10, doi:10.1016/j.cell.2010.03.008.
2. Winterbourn, C. C. The Biological Chemistry of Hydrogen Peroxide. In *Methods in Enzymology*; Elsevier Inc., 2013; Vol. 528, pp. 3–25 ISBN 9780124058811.
3. Ebsworth, E. A. V.; Connor, J. A.; Turner, J. J. The Chemistry of Oxygen. In *Comprehensive Inorganic Chemistry*; Bailar, J. C., Emeléus, H. J., Nyholm, R. S., Trotman-Dickenson, A. F., Eds.; Pergamon Press, 1975; p. 794 ISBN 9781483283135.
4. Gligorovski, S.; Strekowski, R.; Barbati, S.; Vione, D. Environmental Implications of Hydroxyl Radicals ($\bullet\text{OH}$). *Chem. Rev.* **2015**, *115*, 13051–13092, doi:10.1021/cr500310b.
5. Gough, D. R.; Cotter, T. G. Hydrogen peroxide: a Jekyll and Hyde signalling molecule. *Cell Death Dis.* **2011**, *2*, 1–8, doi:10.1038/cddis.2011.96.
6. Moßhammer, M.; Köhl, M.; Koren, K. Possibilities and Challenges for Quantitative Optical Sensing of Hydrogen Peroxide. *Chemosensors* **2017**, *5*, 28, doi:10.3390/chemosensors5040028.
7. Downs, C. A.; Fauth, J. E.; Halas, J. C.; Dustan, P.; Bemiss, J.; Woodley, C. M. Oxidative stress and seasonal coral bleaching. *Free Radic. Biol. Med.* **2002**, *33*, 533–543.
8. Cohen, H. J.; Tape, E. H.; Novak, J.; Chovaniec, M. E.; Liegey, P.; Whitin, J. C. The Role of Glutathione Reductase in Maintaining Human Granulocyte Function and Sensitivity to Exogenous H_2O_2 . *Blood* **1987**, *69*, 493–500.
9. Stone, J. R.; Yang, S. Hydrogen Peroxide: A Signaling Messenger. *Antioxid. Redox Signal.* **2006**, *8*, 243–270, doi:10.1089/ars.2007.1957.
10. Goyen, S.; Pernice, M.; Szabó, M.; Warner, M. E.; Ralph, P. J.; Suggett, D. J. A molecular physiology basis for functional diversity of hydrogen peroxide production amongst Symbiodinium spp. (Dinophyceae). *Mar. Biol.* **2017**, *164*, 1–12, doi:10.1007/s00227-017-3073-5.
11. Abrahamsson, K.; Choo, K.; Pedersén, M.; Johansson, G.; Snoeijs, P. Effects of temperature on the production of hydrogen peroxide and volatile halocarbons by brackish-water algae. *Phytochemistry* **2003**, *64*, 725–734, doi:10.1016/S0031-9422(03)00419-9.
12. Collén, J.; Jiménez Del Río, M.; García-Reina, G.; Pedersén, M. Photosynthetic production of hydrogen peroxide by *Ulva rigida* C. Ag. (Chlorophyta). *Planta* **1995**, *196*, 225–230.
13. Patterson, P. C. O.; Myers, J. Photosynthetic Production of Hydrogen Peroxide by *Anacystis nidulans*. *Plant Physiol.* **1973**, *51*, 104–109.
14. Kalavathi, D. F.; Subramanian, G. Hydrogen Peroxide Photoproduction by A Marine Cyanobacterium *Oscillatoria boryana* BDU 92181 with Potential Use in Bioremediation. *Biosciences Biotechnol. Res. Asia* **2013**, *10*, 929–935.
15. Suggett, D. J.; Warner, M. E.; Smith, D. J.; Davey, P.; Hennige, S.; Baker, N. R. PHOTOSYNTHESIS AND PRODUCTION OF HYDROGEN PEROXIDE BY SYMBIODINIUM (PYRRHOPHYTA) PHYLOTYPES WITH DIFFERENT THERMAL TOLERANCES 1. *J. Phycol.* **2008**, *44*, 948–956, doi:10.1111/j.1529-8817.2008.00537.x.
16. Lesser, M. P. Coral Bleaching: Causes and Mechanisms. In *Coral Reefs: An Ecosystem in Transition*; Dubinsky, Z., Stambler, N., Eds.; Springer Netherlands: Dordrecht, 2011; pp. 405–419 ISBN 978-94-007-0114-4.
17. Tüğsüz, T.; Gök, E.; Ateş, S. Determination of H_2O_2 Content of Various Water Samples Using a Chemiluminescence Technique. *Turkish J. Chem.* **2003**, *27*, 41–47.
18. Febria, C. M.; Lesack, L. F. W.; Gareis, J. A. L.; Bothwell, M. L. Patterns of hydrogen peroxide among lakes of the Mackenzie Delta, western Canadian Arctic. *Can. J. Fish. Aquat. Sci.* **2006**, *63*, 2107–2118, doi:10.1139/F06-

19. King, D. W.; Cooper, W. J.; Rusak, S. A.; Peake, B. M.; Kiddle, J. J.; Sullivan, D. W. O.; Melamed, M. L.; Morgan, C. R.; Theberge, S. M. Flow Injection Analysis of H₂O₂ in Natural Waters Using Acridinium Ester Chemiluminescence: Method Development and Optimization Using a Kinetic Model. *Anal. Chem.* **2007**, *79*, 4169–4176.
20. Cooper, W. J.; Zika, R.; Petasne, R. G.; Plane, J. M. C. Photochemical Formation of H₂O₂ in Natural Waters Exposed to Sunlight. *Environ. Sci. Technol.* **1988**, *22*, 1156–1160.
21. Gonçalves, C.; dos Santos, M. A.; Fornaro, A.; Pedrotti, J. J. Hydrogen Peroxide in the Rainwater of Sao Paulo Megacity: Measurements and Controlling Factors. *J. Braz. Chem. Soc.* **2010**, *21*, 331–339.
22. Jacob, P.; Tavares, T. M.; Rocha, V. C.; Klockow, D. Atmospheric H₂O₂ field measurements in a tropical environment: Bahia, Brazil. *Atmos. Environ.* **1990**, *24A*, 377–382, doi:10.1016/0960-1686(90)90117-6.
23. Zika, R.; Saltzman, E.; Chameides, W. L.; Davis, D. D. H₂O₂ Levels in Rainwater Collected in South Florida and the Bahama Islands. *J. Geophys. Res.* **1982**, *87*, 5015–5017.
24. Kelly, T. J.; Daum, P. H.; Schwartz, S. E. Measurements of Peroxides in Cloudwater and Rain. *J. Geophys. Res.* **1985**, *90*, 7861–7871.
25. Reimer, H. The Daily Changing Pattern of Hydrogen Peroxide in New Zealand. *Environ. Toxicol. Chem.* **1996**, *15*, 652–662.
26. Meslé, M. M.; Beam, J. P.; Jay, Z. J.; Bodle, B.; Bogenschutz, E.; Inskip, W. P. Hydrogen Peroxide Cycling in High-Temperature Acidic Geothermal Springs and Potential Implications for Oxidative Stress Response. *Front. Mar. Sci.* **2017**, *4*, 1–12, doi:10.3389/fmars.2017.00130.
27. Rusak, S. A.; Richard, L. E.; Peake, B. M.; Cooper, W. J. Steady state hydrogen peroxide concentrations across the Subtropical Convergence east of New Zealand. **2005**, 3–4.
28. Yuan, J.; Shiller, A. M. Distribution of hydrogen peroxide in the northwest Pacific Ocean. *Geochemistry Geophys. Geosystems* **2005**, *6*, 1–13, doi:10.1029/2004GC000908.
29. Hopwood, M. J.; Rapp, I.; Schlosser, C.; Achterberg, E. P. Hydrogen peroxide in deep waters from the Mediterranean Sea, South Atlantic and South Pacific Oceans. *Nat. Publ. Gr.* **2017**, 1–10, doi:10.1038/srep43436.
30. Fujiwara, K.; Ushiroda, T.; Takeda, K.; Kumamoto, Y.-I.; Tsubota, H. Diurnal and seasonal distribution of hydrogen peroxide in seawater of the Seto Inland Sea. *Geochem. J.* **1993**, *27*, 103–115.
31. Neftel, A.; Jacob, P.; Klockow, D. Long-term record of H₂O₂ in polar ice cores. **1986**, 262–270.
32. Sigg, A.; Neftel, A. Seasonal variations in hydrogen peroxide in polar ice cores. *Ann. Glaciol.* **1988**, *10*, 157–162.
33. Ho, L. P.; Faccenda, J.; Innes, J. A.; Greening, A. P. Expired hydrogen peroxide in breath condensate of cystic fibrosis patients. *Eur. Respir. J.* **1999**, *13*, 103–106.
34. Sznajder, I. J.; Fraiman, A.; Hall, J. B.; Sanders, W.; Schmidt, G.; Crawford, G.; Nahum, A.; Factor, P.; Wood, L. D. H. Increased Hydrogen Peroxide in the Expired Breath of Patients with Acute Hypoxemic Respiratory Failure. *Clin. Investig. Crit. care* **1969**, *96*, 606–612.
35. Loukides, S.; Horvath, I.; Wodehouse, T.; Cole, P. J.; Barnes, P. J. Elevated Levels of Expired Breath Hydrogen Peroxide in Bronchiectasis. *Am. J. Respir. Crit. Care Med.* **1998**, *158*, 991–994.
36. Long, L. H.; Evans, P. J.; Halliwell, B. Hydrogen Peroxide in Human Urine: Implications for Antioxidant Defense and Redox Regulation. *Biochem. Biophys. Res. Commun.* **1999**, *262*, 605–609.
37. Banerjee, D.; Madhusoodanan, U. K.; Nayak, S.; Jacob, J. Urinary hydrogen peroxide: a probable marker of oxidative stress in malignancy. *Clin. Chim. Acta* **2003**, *334*, 205–209, doi:10.1016/S0009-8981(03)00236-5.
38. Frei, B.; Yamamoto, Y.; Niclas, D.; Ames, B. N. Evaluation of an Isoluminol Chemiluminescence Assay for the Detection of Hydroperoxides in Human Blood Plasma. *Anal. Biochem.* **1988**, *175*, 120–130.

39. Varma, S. D.; Devamanoharan, P. S. Hydrogen Peroxide in Human Blood. *Free Radic. Res. Commun.* **1990**, *14*, 125–131, doi:10.3109/10715769109094124.
40. Giulivi, C.; Hochstein, P.; Davies, K. J. A. Hydrogen Peroxide Production by Red Blood Cells. *Free Radic. Biol. Med.* **1994**, *16*, 123–129.
41. Spector, A.; Garner, W. H. Hydrogen Peroxide and Human Cataract. *Exp. Eye Res.* **1981**, *33*, 673–681.
42. Veal, E. A.; Day, A. M.; Morgan, B. A. Hydrogen Peroxide Sensing and Signaling. *Mol. Cell* **2007**, *26*, 1–14, doi:10.1016/j.molcel.2007.03.016.
43. Yang, J.; Yang, J.; Liang, S. H.; Xu, Y.; Moore, A.; Ran, C. Imaging hydrogen peroxide in Alzheimer's disease via cascade signal amplification. *Sci. Rep.* **2016**, *6*, 35613, doi:10.1038/srep35613.
44. Barnham, K. J.; Masters, C. L.; Bush, A. L. Neurodegenerative diseases and oxidative stress. *Nat. Rev. Drug Discov.* **2004**, *3*, 205–214, doi:10.1038/nrd1330.
45. Yuan, J.; Shiller, A. M. Determination of Subnanomolar Levels of Hydrogen Peroxide in Seawater by Reagent-Injection Chemiluminescence Detection. *Anal. Chem.* **1999**, *71*, 1975–1980, doi:10.1021/ac981357c.
46. Sullivan, D. W. O.; Hanson, A. K.; Kester, D. R. Stopped flow luminol chemiluminescence determination of Fe(II) and reducible iron in seawater at subnanomolar levels. *Mar. Chem.* **1995**, *49*, 65–77.
47. Price, D.; Mantoura, R. F. C.; Worsfold, P. J. Shipboard determination of hydrogen peroxide in the western Mediterranean sea using flow injection with chemiluminescence detection. *Anal. Chim. Acta* **1998**, *371*, 205–215.
48. Cooper, W. J.; Moegling, J. K.; Kieber, R. J.; Kiddle, J. J. A chemiluminescence method for the analysis of H₂O₂ in natural waters. *Mar. Chem.* **2000**, *70*, 191–200.
49. Miller, G. W.; Morgan, C. A.; Kieber, D. J.; King, D. W.; Snow, J. A.; Heikes, B. G.; Mopper, K.; Kiddle, J. J. Hydrogen peroxide method intercomparison study in seawater. *Mar. Chem.* **2005**, *97*, 4–13, doi:10.1016/j.marchem.2005.07.001.
50. Morris, J. J.; Johnson, Z. I.; Wilhelm, S. W.; Zinser, E. R. Diel regulation of hydrogen peroxide defenses by open ocean microbial communities. *J. Plankton Res.* **2016**, *38*, 1103–1114, doi:10.1093/plankt/fbw016.
51. Schneider, R. J.; Roe, K. L.; Hansel, C. M.; Voelker, B. M. Species-Level Variability in Extracellular Production Rates of Reactive Oxygen Species by Diatoms. *Front. Chem.* **2016**, *4*, 1–13, doi:10.3389/fchem.2016.00005.
52. Valeur, B. *Molecular Fluorescence: Principles and Applications*; Wiley-VCH, 2001; ISBN 3-527-29919-X.
53. Torto, N.; Mwatseteza, J.; Laurell, T. Microdialysis Sampling - Challenges and New Frontiers. *LC GC Eur.* **2001**, 1–6.
54. de Lange, E. C. M. Recovery and Calibration Techniques: Toward Quantitative Microdialysis. In *Microdialysis in Drug Development*; Müller, M., Ed.; 2013; Vol. 4, pp. 3–12 ISBN 978-1-4614-4814-3.
55. Nandi, P.; Lunte, S. M. Recent trends in microdialysis sampling integrated with conventional and microanalytical systems for monitoring biological events: A review. *Anal. Chim. Acta* **2009**, *651*, 1–14, doi:10.1016/j.aca.2009.07.064.
56. Hassett, D. J.; Ma, J. F.; Elkins, J. G.; McDermott, T. R.; Ochsner, U. a; West, S. E.; Huang, C. T.; Fredericks, J.; Burnett, S.; Stewart, P. S.; McFeters, G.; Passador, L.; Iglewski, B. H. Quorum sensing in *Pseudomonas aeruginosa* controls expression of catalase and superoxide dismutase genes and mediates biofilm susceptibility to hydrogen peroxide. *Mol. Microbiol.* **1999**, *34*, 1082–1093, doi:DOI 10.1046/j.1365-2958.1999.01672.x.
57. Miller, G. W.; Morgan, C. A.; Kieber, D. J.; King, D. W.; Snow, J. A.; Heikes, B. G.; Mopper, K.; Kiddle, J. J. Hydrogen peroxide method intercomparison study in seawater. *Mar. Chem.* **2005**, *97*, 4–13, doi:10.1016/j.marchem.2005.07.001.
58. King, D. W.; Cooper, W. J.; Rusak, S. A.; Peake, B. M.; Kiddle, J. J.; O'Sullivan, D. W.; Melamed, M. L.; Morgan, C. R.; Theberge, S. M. Flow Injection Analysis of H₂O₂ in Natural Waters Using Acridinium Ester Chemiluminescence: Method Development and Optimization Using a Kinetic Model. *Anal. Chem.* **2007**, *79*, 4169–4176, doi:10.1021/ac062228w.

59. Holzgrabe, U.; Borst, C.; Büttner, C.; Bitar, Y. Quantitative Analysis in Pharmaceutical Analysis. In *Chiral Separations by Capillary Electrophoresis*; Van Eeckhaut, A., Michotte, Y., Eds.; CRC Press, 2009; p. 543 ISBN 978-1-4200-6933-4.
60. Appendix B ICH Guidelines on Validation of Analytical Procedures. In *A Laboratory Quality Handbook of Best Practice*; Singer, D. C., Ed.; ASQ Quality Press, 2001; p. 404 ISBN 0-87389-491.
61. Koren, K.; Jensen, P. Ø.; Kühl, M. Development of a rechargeable optical hydrogen peroxide sensor – sensor design and biological application. *Analyst* **2016**, *141*, 4332–4339, doi:10.1039/C6AN00864J.
62. Grajales, A.; Rodríguez, E. Morphological revision of the genus *Aiptasia* and the family Aiptasiidae (Cnidaria, Actiniaria, Metridioidea). *Zootaxa* **2014**, *3826*, 55–100, doi:10.11646/zootaxa.3826.1.2.
63. Hoegh-Guldberg, O.; Bruno, J. F. The Impact of Climate Change on the World's Marine Ecosystems. *Science* (80-.). **2010**, *328*, 1523–1529, doi:10.1126/science.1189930.
64. Voolstra, C. R. A journey into the wild of the cnidarian model system *Aiptasia* and its symbionts. *Mol. Ecol.* **2013**, *22*, 4366–4368, doi:10.1111/mec.12464.
65. King, D. W.; Lounsbury, H. A.; Millero, F. J. Rates and Mechanism of Fe(II) Oxidation at Nanomolar Total Iron Concentrations. *Environ. Sci. Technol.* **1995**, *29*, 818–824, doi:10.1021/es00003a033.
66. King, D. W. Role of carbonate speciation on the oxidation rate of Fe(II) in aquatic systems. *Environ. Sci. Technol.* **1998**, *32*, 2997–3003, doi:10.1021/es980206o.
67. Emmenegger, L.; King, D. W.; Sigg, L.; Sulzberger, B. Oxidation kinetics of Fe(II) in a eutrophic swiss lake. *Environ. Sci. Technol.* **1998**, *32*, 2990–2996, doi:10.1021/es980207g.
68. Kustka, A. B.; Shaked, Y.; Milligan, A. J.; King, D. W.; Morel, F. M. M. Extracellular production of superoxide by marine diatoms: Contrasting effects on iron redox chemistry and bioavailability. *Limnol. Oceanogr.* **2005**, *50*, 1172–1180, doi:10.4319/lo.2005.50.4.1172.
69. Rose, A. L.; Moffett, J. W.; Waite, T. D. Determination of superoxide in seawater using 2-methyl-6-(4-methoxyphenyl)-3,7-dihydroimidazo[1,2-a]pyrazin-3(7H)-one chemiluminescence. *Anal. Chem.* **2008**, *80*, 1215–1227, doi:10.1021/ac7018975.
70. Garg, S.; Rose, A. L.; Godrant, A.; Waite, T. D. Iron uptake by the ichthyotoxic *Chattonella marina* (Raphidophyceae): Impact of superoxide generation. *J. Phycol.* **2007**, *43*, 978–991, doi:10.1111/j.1529-8817.2007.00394.x.